Thermosolvatochromism of Betaine-30 in CH_3CN

Xihua Zhao, Jim A. Burt, Fritz J. Knorr, and Jeanne L. McHale*

Department of Chemistry, University of Idaho, Moscow, Idaho 83844-2343

Received: July 13, 2001; In Final Form: September 27, 2001

The solvatochromic dye betaine-30 is thermochromic as well, due to the temperature dependence of solvent polarity, which strongly influences the wavelength of the visible absorption band. We report an analysis of the temperature-dependent absorption spectrum of betaine-30 in CH_3CN, incorporating the internal-mode displacements determined from the resonance Raman profiles at room temperature. The temperature-dependent solvent reorganization energy λ_{solv} associated with the visible transition of betaine-30 influences the width and position of the absorption spectrum and is relevant to theories for the rate of return electron transfer. We have previously determined λ_{solv} for betaine-30 in acetonitrile and deuterated acetonitrile from analysis of the room-temperature absorption and resonance Raman profiles using time-dependent spectroscopy theory. In this work, we present a revised set of normal-mode displacements, including the contribution from a torsional mode of betaine-30 at 133 cm^{-1}, obtained from an analysis of the room-temperature Raman profiles in CH_3CN and CD_3CN. These displacements are then kept fixed, and the temperature-dependent absorption spectrum of betaine-30 in acetonitrile is modeled to obtain the solvent reorganization energy, 0−0 energy, and transition moment as a function of temperature. The solvent reorganization energy λ_{solv} is found to decrease with increasing temperature, consistent with decreasing solvent polarity but opposite to the prediction of dielectric continuum theory. In contrast to our previous analysis, the nonlinear solvent response is included in the model, and the amplitude of the solvent response is found to be smaller in the excited than the ground electronic state, due to the decrease in solute dipole moment in the excited electronic state.

I. Introduction

The highly solvatochromic molecule betaine-30 (Scheme 1) has been widely applied as a solvent polarity probe[1] and has been used to investigate solvent effects on the rate of back-electron transfer (nonradiative relaxation) following charge-transfer excitation.[2] The solvent sensitivity of this probe derives from the much larger dipole moment in the ground state than the excited state; hence, increasing solvent polarity results in a blue shift in the charge transfer transition. We previously examined the room-temperature absorption and resonance Raman excitation profiles of betaine-30 in acetonitrile[3a] and methanol[3b] and their deuterated derivatives to investigate the solvent and internal-mode dynamics which couple to the visible electronic transition. Analysis of the experimental line shapes using time-dependent theory enabled the solvent and internal reorganization energies, λ_{solv} and λ_{int}, to be determined. These quantities, which represent the energy difference of the electronically excited chromophore in the vertical and relaxed configurations, contribute to the expression for the rate of back-electron transfer, k_{et}, and continue to be of interest in the theory of electron transfer.

Figures 1 and 2 show the resonance Raman spectrum of betaine-30 in acetonitrile and acetonitrile-d_3, respectively. In ref 3a, we reported the results of modeling the resonance Raman and absorption profiles of betaine-30 in these two solvents using time-dependent theory. In that work, we found the solvent reorganization energy to be much larger than the prediction of classical continuum theory, which treats the solvent as a structureless medium characterized by the bulk dielectric constant and refractive index. The failures of continuum theory are well-known,[4] and it is not surprising that a very solvent-sensitive probe such as betaine-30 would report short-range solvation effects not included in the classical theory. However, as stated in ref 3a, our fitted values for λ_{solv} (about 6000 cm^{-1}) were overestimated due to neglect of internal vibrational modes overlapped by solvent lines in either CH_3CN or CD_3CN solution, as shown in Figures 1 and 2. Our interest at the time was to compare solvent dynamics in the two systems, so we included the same number of normal modes in the analysis of both systems. Recent quantum calculations and normal-mode analysis of betaine-30 suggest that a torsional mode at 133 cm^{-1}, in which the pyridyl and phenolate rings undergo relative internal rotation, is also strongly coupled to the lowest energy transition.[5] This low-frequency mode is obscured by Rayleigh scattering from the solvent in acetonitrile solution, though it has been observed in propylene carbonate solution as reported in ref 5. To obtain a more accurate estimate of λ_{solv}, we reevaluate the Raman excitation profiles in CH_3CN and CD_3CN solution in

SCHEME 1: Structure of Betaine-30

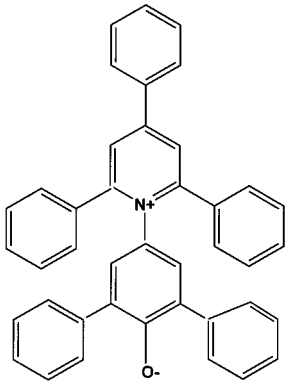

10.1021/jp012699g CCC: $20.00 © 2001 American Chemical Society
Published on Web 11/08/2001

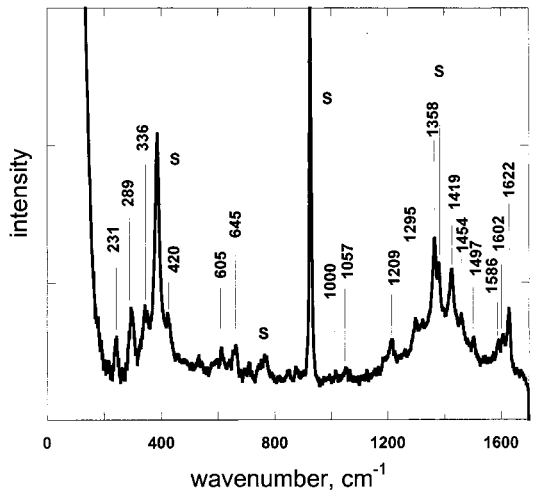

Figure 1. Resonance Raman spectrum of betaine-30 in CH_3CN, excited at 634 nm. Solvent lines are marked with "S."

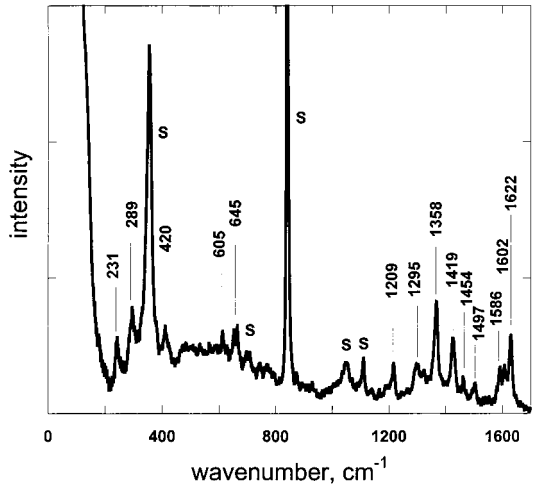

Figure 2. Resonance Raman spectrum of betaine-30 in CD_3CN, excited at 634 nm. Solvent lines are marked with "S."

the present study using a more complete set of 19 betaine-30 modes, the displacements for which are constrained to be the same in both solvent isotopomers. The solvent isotope effects on the Raman intensities are accounted for by slightly different solvent reorganization energies in CH_3CN and CD_3CN. These displacements are then employed in modeling the temperature-dependent absorption spectrum in CH_3CN.

Solvent and internal reorganization energies contribute to the width and position of the absorption profile. The average absorption frequency $\bar{\nu}$, equal to the peak frequency for a symmetric band, is given by

$$h\bar{\nu} \equiv h\int \nu I(\nu)\, \mathrm{d}\nu = E_0 + \lambda_{\mathrm{int}} + \lambda_{\mathrm{solv}} \qquad (1)$$

where E_0 is the origin of the transition, and the normalized intensity $I(\nu)$ is proportional to the measured absorption cross section $\sigma_A(\nu)$ divided by the frequency. The width of the absorption spectrum also increases with increasing values of λ_{solv} and λ_{int}. Each intramolecular vibrational mode contributes λ_a to the internal reorganization energy in proportion to the square of the dimensionless displacement Δ_a of the excited-state potential along the normal coordinate Q_a

$$\lambda_{\mathrm{int}} = \sum_a \lambda_a = \frac{1}{2}\sum_a \Delta_a{}^2 h\nu_a \qquad (2)$$

where ν_a is the frequency of the mode. Though absorption band shapes of dyes are often fit using one or a few internal modes, this procedure is necessarily ambiguous when the vibrational structure is not resolved, and for betaine-30, this procedure is at odds with the large number of normal modes which contribute to the resonance Raman spectrum[3]. However, since the resonance Raman activity also depends on the displacements Δ_a and on the solvent reorganization energy, simultaneous modeling of the absorption and resonance Raman profiles enables the internal and solvent reorganization energies to be separated.[6] While increasing solvent reorganization energy broadens the absorption spectrum with no change in band area, the effect on the Raman profiles is to decrease the intensity. Increasing internal reorganization energy along a given normal coordinate, on the other hand, results in greater Raman intensity.

In the present work, we also take advantage of the temperature dependence of the absorption spectrum, which for the most part reflects changes in solvent rather than internal reorganization energy, to accomplish this separation. As has been previously reported,[1,2c,7] the decrease in solvent polarity with increasing temperature results in a red shift of the $S_0 \rightarrow S_1$ (charge-transfer) transition of betaine-30. Internal modes which are high in frequency compared to thermal energy, $h\nu_a \gg k_B T$, make little contribution to the temperature dependence of the width and position of the absorption spectrum. The solvent reorganization energy and E_0, on the other hand, are both expected to decrease as the solvent becomes less polar, accounting for the red shift of the absorption maximum as temperature increases. Thus we can employ the thermochromism of betaine-30 and modeling of the absorption line shape using time-dependent theory to evaluate the solvent reorganization energy as a function of temperature. Here, we employ the room-temperature Raman cross sections of betaine-30 in CH_3CN and CD_3CN to obtain a set of normal-mode displacements which are constrained to be the same in both solvents, independent of temperature. These are then employed in an analysis of the temperature-dependent absorption line shape to obtain the temperature-dependent values of E_0, the transition moment, and the (ground state) reorganization energy.

The determination of λ_{solv} depends on a model for the solvent-induced dephasing of the electronic transition. As in previous work, we treat the influence of the solvent on the electronic transition with the Brownian oscillator model of Mukamel and co-workers.[8] In this approach, the time-correlation function $M(t)$ for the solvent-induced fluctuations in the transition frequency is taken to be an exponential function:

$$M(t) \equiv \frac{\langle \delta\omega_{\mathrm{ge}}(t)\delta\omega_{\mathrm{ge}}(0)\rangle}{D^2} = \exp(-\Lambda t) \qquad (3)$$

where $\delta\omega_{\mathrm{ge}}(t) = \omega_{\mathrm{ge}}(t) - \langle\omega_{\mathrm{ge}}\rangle$ is the time-dependent fluctuation in the electronic transition frequency compared to the average value, $D \equiv \langle(\delta\omega_{\mathrm{ge}})^2\rangle^{1/2}$ is the amplitude, and Λ is the rate at which the correlations in these fluctuations relax. The angle brackets indicate an equilibrium average which, in the case of linear solvent response (as is assumed by the Brownian oscillator model), is independent of the electronic state of the solute. The physical picture behind this model is that the electronic transition is coupled to a solvent mode which is displaced in the excited electronic state with no change in frequency. These assumptions lead to a simple closed form expression for the dephasing function, $\exp[-g(t)]$, the Fourier transform of which is the contribution of the solvent to the absorption line shape. The resonance Raman profile (Raman cross section as a function of

frequency) is also dependent on the dephasing function, and it is convenient to assume linear solvent response so that the same function can be used to simultaneously model the absorption and Raman profiles with a common $g(t)$. Our previous work employed the overdamped Brownian oscillator model in the high-temperature and high-damping limit. In the present work, we use a more general expression for $g(t)$ (eqs 26−29 of ref 8b) which is valid at arbitrary temperature and avoids anomalous (negative) absorption, which is sometimes obtained using the high-temperature form of the model.[8,9]

In the present study, we account for the nonlinear solvent response which is evidenced by our data for the absorption and resonance Raman profiles of betaine-30 in CH_3CN and CD_3CN. Though the absorption spectrum is independent of solvent isotopomer, the Raman intensities are generally greater in CH_3CN than in CD_3CN. Since it is unlikely that the excited-state geometry of the solute depends on solvent isotopic substitution, the Raman intensities reveal that solvent dynamics coupled to the excited electronic state are different in CH_3CN and CD_3CN. The absorption spectrum, however, indicates that the solvent dynamics coupled to the ground electronic state are the same in CH_3CN and CD_3CN. The average represented by the angle brackets in eq 3 is therefore dependent on the electronic state of the solute in this system, a result of the large change in dipole moment that accompanies excitation. In the case of the absorption profile, $M(t)$ accounts for solvent motion equilibrated to the ground state dipole moment of the solute, and this motion is apparently little different in CH_3CN and CD_3CN. The Raman intensities, on the other hand, depend on initial configurations of the solvent which are far from equilibrium, and different dynamics in protio- and deuteroacetonitrile result in different averages for $M(t)$. If we view the solvent response in terms of a reorientational solvent mode coupled to the transition, the frequency of this mode is expected to decrease when the solute is excited to the less polar excited electronic state, and (as will be shown below) the result is a smaller solvent reorganization energy when the solvent is coupled to the excited rather than the ground electronic state of the solute.

II. Experimental Section

Betaine-30 was purchased from Aldrich and recrystallized from methanol/water 3:1 (v/v), followed by chromatography on a basic alumina column using 1:1 ethyl acetate/petroleum ether. This treatment is necessary to remove a strongly fluorescecent impurity present in the material as received. HPLC acetonitrile was distilled before use and dried over molecular sieves. Spectra were recorded in thermostated 1 cm cells at 0.1 nm resolution using a Shimadzu U-2501 spectrometer. The uncertainty in the temperature measurement is estimated to be ±0.5 °C. Absorption spectra were corrected to the concentration at 20 °C using temperature-dependent density parameters of ref 10. The temperature-dependent dielectric constant ϵ_s of acetonitrile was found using the equation $\epsilon_s(T) = a + bT + cT^2$ and the parameters $a = 297.2$, $b = -1.55$ K^{-1}, and $c = 0.002259$ K^{-2} from ref 11. The refractive index of acetonitrile was taken to be a linearly decreasing function of temperature, using the slope $dn/dT = -0.0045$ K^{-1} from ref 12. The Raman spectra shown in Figures 1 and 2 were obtained with 80 mW of power at 634 nm, using 90° scattering and a solution concentration of 7×10^{-4} M. Experimental details for the Raman profiles shown in Figure 4 are given in ref 3a.

An optimization algorithm based on eqs 8 and 9 was used to model the room-temperature Raman excitation profiles of betaine-30 in acetonitrile and perdeuterated acetonitrile and the temperature-dependent absorption spectrum in acetonitrile, as discussed below. Simplex and Levenberg−Marquardt algorithms were alternately used to minimize the χ^2 error between the calculated and experimental spectra. The parameters that were varied included the transition moment, the band origin, mode displacements, and the solvent reorganization energy, as described in the next section. The spectra were fit between 12 500 and 18 000 cm^{-1}. The spectra were not fit beyond 18 000 cm^{-1} to avoid contributions from a higher-energy transition in the ultraviolet. The time-dependent overlap integrals were evaluated using formulas in ref 8a, which depend on the 0−0 energy, E_0, the ground and excited-state vibrational frequencies, and dimensionless displacements for each mode. The ground-state vibrational frequencies for 19 Raman active modes, assumed to be the same in the excited electronic state, were taken from ref 3a. The program varied displacements for the nine modes for which excitation profiles are shown in Figure 4. Displacements for the remaining modes were manually adjusted by comparing the calculated Raman spectrum at 605 nm excitation with the spectrum in ref 3a. The 133 cm^{-1} mode displacement was determined by comparison with the Raman spectrum in ref 5b. The first overtone of the 133 cm^{-1} mode was calculated to ensure it was not observable as indicated by the data. Thermally excited initial states were included by permitting the following maximum vibrational quantum numbers to contribute to the sum in eqs 8 and 9: up to $v = 3$ for the 133 cm^{-1} mode, $v = 2$ for the 231 cm^{-1} mode, and $v = 1$ for the 289 and 320 cm^{-1} modes. Including these thermally populated states was found not to have a big effect on the calculated absorption spectrum, but it did influence the Raman profiles. The solvent dephasing model of Li et al.[8b] was used for $\exp[-g(t)]$.

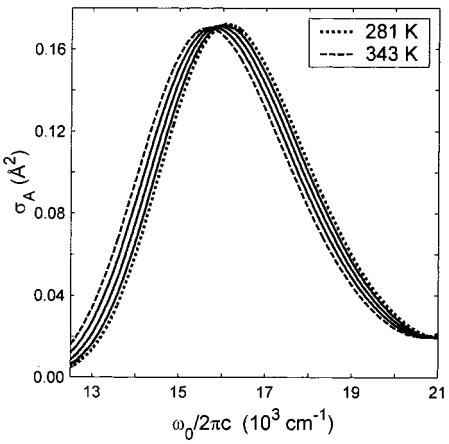

Figure 3. Absorption spectrum of betaine-30 in acetonitrile at temperatures 281, 292, 308, 325, and 343, corrected to the density at 20 °C. The spectrum shifts to the red as temperature increases.

III. Results

The temperature-dependent absorption spectrum of betaine-30 in CH_3CN is shown in Figure 3. The data have been corrected to the absorbance expected for the density (concentration) of the solution at 20 °C. There is a clear red shift and slight increase in integrated intensity as the temperature is raised, but no evidence for an isosbestic point. The absorption maximum shifts from 622 to 640 nm (a red shift of about 450 cm^{-1}) and the full-width at half-maximum increases from 4010 to 4100 cm^{-1} as the temperature is raised from 8 to 70 °C. The data suggest that the thermochromism results from the decrease in solvent reorganization energy and E_0 as temperature is raised. Treating the solvent as a dielectric continuum,[13] the solvent reorganization

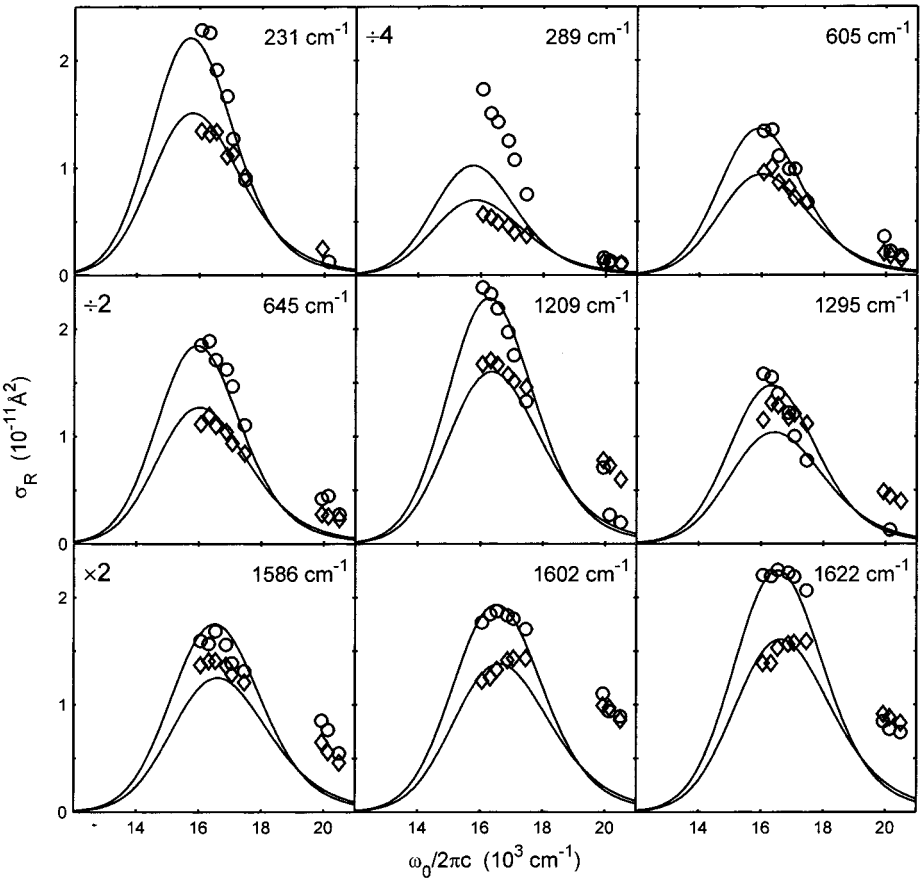

Figure 4. Experimental (points) and calculated (lines) Raman excitation profiles for betaine-30 in CH_3CN (circles) and CD_3CN (diamonds) at room temperature.

energy in wavenumbers is estimated using eq 4:

$$\lambda_{\text{solv}} = \frac{(\Delta\mu)^2}{hca^3}\left[\frac{\epsilon_s - 1}{2\epsilon_s + 1} - \frac{n^2 - 1}{2n^2 + 1}\right] \tag{4}$$

where $\Delta\mu = \mu_e - \mu_g$ is the difference in the ground and excited-state dipole moments, a is the cavity radius, ϵ_s is the static dielectric constant, n is the refractive index, h is Planck's constant, and c is the speed of light. The dipole moment of betaine-30 has been reported to decrease from 15 D in the ground state to 6 D in the excited state.[14] Assuming that the ground and excited-state dipole moments are parallel ($\Delta\mu = 9$ D) and using a cavity radius of 6 Å, along with the temperature-dependent static and optical dielectric constants, the solvent reorganization energy is predicted to increase from about 540 cm^{-1} at 7 °C to 760 cm^{-1} at 70 °C, a blue shift of 220 cm^{-1}. This contrasts with the observed red shift of 450 cm^{-1} over this temperature range. There is considerable uncertainty in the direction of the ground and excited-state dipole moments, as discussed further in Section IV. If the ground and excited-state dipole moments are taken to be antiparallel ($\Delta\mu = 21$ D), an even larger blue shift of 1200 cm^{-1} is predicted. Regardless of the uncertainty in the continuum prediction due to the choice of cavity radius, the direction of the excited state dipole, and the rather crude assumption that the refractive index is linear in temperature, it is clear that the continuum expression cannot account for the observed red shift in the absorption spectrum with increasing temperature. It has been previously noted that dielectric continuum theory predicts incorrect temperature dependence of λ_{solv} in other charge-transfer systems,[4b,c] as is the case here.

The origin of the transition E_0 may also depend on temperature. Following ref 13, the continuum theory expression for E_0 in solution is

$$E_0 = E_0(\text{gas}) + \left(\frac{\mu_g^2 - \mu_e^2}{a^3}\right)\left(\frac{\epsilon_s - 1}{2\epsilon_s + 1}\right) \tag{5}$$

The above equation predicts that E_0 should decrease by 25 cm^{-1} as the temperature is raised. This prediction is independent of the uncertainties in the directions of μ_g and μ_e and in the temperature dependent refractive index. Again, continuum theory does not even qualitatively account for the observed thermochromism, as has been noted in studies on other charge-transfer systems.[4]

In our previous study, we simulated the absorption and Raman profiles using time-dependent theory and Mukamel's Brownian oscillator model for the solvent-induced dephasing[8] and found the line shape to be in the inhomogeneous limit ($\Lambda < < D$). The solvent contribution to the line shape, essentially a Gaussian function, is determined by the amplitude D of the solvent-induced frequency fluctuations, which also contributes to the solvent reorganization energy:

$$\lambda_{\text{solv}} = \frac{D^2}{2k_B T} \tag{6}$$

where k_B is Boltzmann's constant. In the inhomogeneous limit, the solvent contribution to the line shape is a Gaussian with full-width at half-height: $\Delta\nu_{1/2} \approx 2.355D$. If the amplitude D were independent of temperature, the solvent reorganization energy would decrease as temperature is increased, causing a

red shift in agreement with experiment. The relatively small increase in line width, however, about 100 cm^{-1} from 8 to 70 °C, suggests there is a slight increase in amplitude, expected as the thermal motion of the solvent increases and density decreases.

Low-frequency internal modes also contribute to the temperature dependence of the line width:[13]

$$\Delta\nu_{1/2} = 1.67\sum_a \Delta_a \nu_a \left[\coth\left(\frac{h\nu_a}{2k_B T}\right)\right]^{1/2} \quad (7)$$

where the sum in eq 7 runs over modes having dimensionless displacements Δ_a and frequencies ν_a. Considering the torsional mode at 133 cm^{-1} as a likely candidate, a displacement as large as $\Delta_a = 1.0$ would contribute ~390 cm^{-1} to the half-width at 8 °C and 430 cm^{-1} at 70 °C. The observed increase in line width with temperature probably reflects both solvent and low-frequency internal mode contributions, which are not simply additive. We therefore model the room-temperature Raman profiles of betaine-30 in CH_3CN and CD_3CN (from ref 3a) and the variable-temperature absorption data in CH_3CN using time-dependent theory and a common set of normal mode displacements, considered the same in both solvent isotopomers and independent of temperature.

As in our previous studies, the time-dependent formalism of Heller[15] is employed to calculate the absorption cross section:

$$\sigma_A(\omega_0) = \frac{2\pi(\mu_{ge})^2\omega_0}{3\hbar cn}\sum_i P_i \int_{-\infty}^{\infty}\langle i|i(t)\rangle \exp[i(\omega_0 + \omega_i)t] \exp[-g(t)]\, dt \quad (8)$$

where ω_0 is the incident frequency, P_i is the probability that initial state i is occupied, μ_{ge} is the transition moment, $\hbar\omega_i$ is the energy of the initial state, $|i(t)\rangle$ is the multimodal initial vibrational state propagating on the upper potential surface, and the function $\exp[-g(t)]$ accounts for the solvent-induced dephasing. The time-dependent overlaps $\langle i|i(t)\rangle$ are evaluated by assuming separable harmonic oscillator vibrational states with equal frequency in the ground and excited electronic states. The Raman cross section for the $i \rightarrow f$ transition is given by

$$\sigma_R(\omega_0) = \frac{8\pi\omega_0\omega_s^3(\mu_{ge})^4}{9\hbar^2c^4}\sum_i P_i \left|\int_0^{\infty}\langle f|i(t)\rangle \exp[i(\omega_0 + \omega_i)t] \exp[-g(t)]\, dt\right|^2 \quad (9)$$

where ω_s is the frequency of the scattered light and the time-evolving initial state $|i(t)\rangle$ is projected onto the time-zero final state $\langle f|$. In our previous work, we allowed the transition moment to contain terms linear in the normal coordinates, but these non-Condon effects are neglected in the present study.

As shown in Figure 4, the Raman intensities are generally higher in CH_3CN than in CD_3CN, even though the absorption spectrum is independent of solvent isotopic substitution. In the analysis of ref 3a, we obtained a best fit to the room-temperature absorption and Raman profiles of betaine-30 in CH_3CN using the following parameters: $E_0 = 9850$ cm^{-1}, $\mu_{ge} = 3.7$D, $D = 1570$ cm^{-1}, and the nine normal-mode frequencies and displacements listed in Table 2 of ref 3a. With this set of data the solvent and internal reorganization energies were found to be 5980 and 120 cm^{-1}, respectively. When the displacements and the amplitude D are held constant and the absorption profiles calculated at temperatures between 280 and 340 K, the simulated spectra displayed a much larger red shift than was observed experimentally. This suggests that our previous estimate of D and thus λ_{solv} was too large, due to the neglect of betaine-30 vibrational modes overlapped by solvent bands. In addition, the torsion at 133 cm^{-1} was not included, though it is reported[5] to have a relative intensity half as strong as the most intense vibration of betaine-30. We therefore repeated the modeling with the addition of the 133 cm^{-1} mode and nine previously neglected modes.

TABLE 1: Displacements Δ_a Obtained from Analysis of the Room Temperature Raman Profiles of Betaine-30 in CH_3CN and CD_3CN, Using $E_0 = 12\,100$ cm^{-1}, $\mu_{ge} = 3.96$ D, and λ_{solv}(ram) = 3320 cm^{-1} (in CH_3CN) and 3690 cm^{-1} (in CD_3CN)

$\tilde{\nu}_a$, cm^{-1}	Δ_a	$\tilde{\nu}_a$, cm^{-1}	Δ_a
133	0.700	1209	0.081
231	0.350	1295	0.062
289	0.388	1358	0.075
336	0.270	1419	0.065
420	0.140	1454	0.028
605	0.116	1497	0.028
645	0.180	1586	0.041
1000	0.012	1602	0.061
1057	0.014	1622	0.065
1181	0.030		

In ref 3a, we employed the same solvent dephasing function $g(t)$ in the calculation of both the absorption and Raman cross sections. This resulted in normal-mode displacements which differed for betaine-30 in CH_3CN versus CD_3CN. In this study, we permit the solvent dephasing parameters to differ for the calculation of the absorption and Raman profiles, and in the Raman case, we permit these parameters to differ for CH_3CN and CD_3CN. A single set of mode displacements is employed to reproduce all the spectra, including the temperature-dependent absorption profiles. In this approach, the solvent reorganization energies are interpreted as follows:

$$\lambda_{solv}(\text{abs}) = \frac{\langle(\delta\omega_{ge})^2\rangle_g}{2k_B T} \quad (10a)$$

$$\lambda_{solv}(\text{ram}) = \frac{\langle(\delta\omega_{ge})^2\rangle_e}{2k_B T} \quad (10b)$$

where the subscript on the angle brackets indicates an average over the ground or excited state of the solute.

We first simultaneously modeled the (room temperature) absorption spectrum in acetonitrile and the Raman profiles in CH_3CN and CD_3CN, constraining the mode displacements but not the solvent dephasing parameters to be the same in all three data sets. The mode displacements obtained from this global analyis were then fixed, and the absorption spectrum was modeled at nine temperatures between 281 and 343 K. Best fits to the experimental Raman profiles are shown in Figure 4. The calculation incorporated normal-mode displacements for 19 betaine-30 modes, shown in Table 1, as well as common values of E_0 (12 120 cm^{-1}) and μ_{ge} (3.95 D), for both protiated and deuterated acetonitrile. The values for Λ and λ_{solv}, on the other hand, were allowed to vary with solvent isotopomer. The calculated Raman profiles in Figure 4 were obtained using λ_{solv}(ram) values of 3320 and 3690 cm^{-1} in CH_3CN and CD_3CN, respectively. The fitted values of the frequency Λ were found to be about 100 and 200 cm^{-1} in protiated and deuterated solvent, respectively. The calculated spectra are much more sensitive to λ_{solv} than to Λ, so the fitted values for the frequency should not be overinterpreted. With the exception of the 289

TABLE 2: Solvent Reorganization Energy λ_{solv}, Transition Moment μ_{ge}, and 0−0 Energy E_0 Obtained by Applying Time-Dependent Theory to the Temperature-Dependent Absorption Spectrum of Betaine-30 in CH_3CN[a]

temp, K	λ_{solv}, cm^{-1}	μ_{ge}, D	E_0, cm^{-1}
281	4560	3.90	12,060
285	4540	3.90	12,050
292	4510	3.91	12,020
300	4490	3.92	11,960
308	4470	3.93	11,910
317	4440	3.94	11,870
325	4420	3.95	11,820
334	4390	3.96	11,780
343	4360	3.97	11,730

[a] The reported transition moments neglect the temperature dependence of the refractive index (see text).

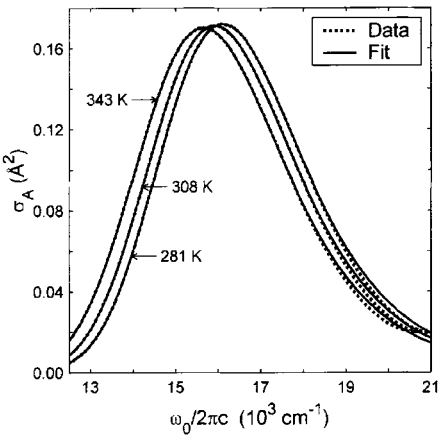

Figure 5. Experimental (dashed line) and calculated (full line) absorption spectrum of betaine-30 in acetonitrile at 281, 308, and 343 K.

cm^{-1} mode, the model does a good job of accounting for the solvent isotope effect on the Raman intensities. The total internal reorganization energy for the 19 betaine-30 modes was found to be 122 cm^{-1}.

We next modeled the absorption spectrum as a function of temperature, keeping the mode displacements fixed, but varying μ_{ge}, E_0, and the solvent dephasing parameters at each temperature to get the best fit. The values of E_0 and μ_{ge} used to simulate the room-temperature absorption spectrum were not constrained to be the same as those found from the global analysis, but the values obtained by optimizing the fit to the absorption alone at 292 K (12 020 cm^{-1} and 3.91 D) were only slightly different from those obtained by simultaneously modeling the Raman and absorption profiles (12 100 cm^{-1} and 3.96 D). Table 2 shows the temperature-dependent parameters found from fitting the absorption data, and the calculated and experimental absorption spectra are compared at three temperatures in Figure 5. The optimized value of Λ was close to 370 cm^{-1} (to within a few wavenumbers) at all temperatures, with no definite trend. The fitted value of the transition moment, which parallels the temperature dependence of the integrated absorbance, is found to show a slight increase from 3.90 D at 281 K to 3.97 D at 343 K. To avoid uncertainty in the temperature-dependent refractive index, the transition moments reported in Table 2 are based on a refractive index fixed at the room-temperature value of 1.34. (The absorption spectrum is scaled by μ_{ge}^2/n.) If the estimated decrease in refractive index with temperature is accounted for, assuming that n is a linear function of temperature with $dn/dT = -.0045\ K^{-1}$, the fitted transition moment ranges from 4.0 D at 281 K to 3.7 D at 343 K. This assumption probably overestimates the temperature dependence of the refractive index and therefore also that of the transition moment. The intensity of the $S_0 \rightarrow S_1$ transition of betaine-30 is larger in less polar environments, according to calculations[16] and experiments,[1] so the transition moment is expected to increase with temperature. The origin of the transition E_0 drops from 12 060 cm^{-1} at 281 K to 11 730 cm^{-1} at 341 K, a much larger decrease than that predicted by continuum theory (eq 5). The solvent reorganization energy decreases from 4560 to 4360 cm^{-1} over this temperature range, corresponding to an amplitude D which increases from 1330 to 1440 cm^{-1}. The temperature dependence of the fitted parameters for the absorption spectrum of betaine-30 in acetonitrile is consistent with the conclusion that the spectral changes are a consequence of solvent polarity which decreases with increasing temperature.

TABLE 3: Comparison of Room-Temperature Values of the Band Origin E_0, Solvent Reorganization Energy λ_{solv} for Absorption, Classical Reorganization Energy λ_{class}, Internal Reorganization Energy λ_{int}, and Transition Moment μ_{ge} for Betaine-30 in Acetonitrile Found in This Work and Others

	E_0, cm^{-1}	λ_{solv}, cm^{-1}	λ_{class}, cm^{-1}	λ_{int}, cm^{-1}	μ_{ge}, D
this work	12020	4510		120	3.9
Rossky[a]	13753	3625	760		2.1
Maroncelli[b]	11710	4260	1100		
Barbara[c]	11645	2221	1233	1236	

[a] Ref 16a. [b] Ref 17. [c] Ref 2a.

IV. Discussion

Table 3 compares our derived values of the band origin, reorganization energies (for absorption) and transition moment at room temperature to those reported in other work. In some of these reports, it is possible to distinguish a classical reorganization energy λ_{class} due to low-frequency intramolecular vibrations, such as torsions, from that due just to solvent reorganization, which is also treated classically. Lobaugh and Rossky (LR) have pointed out some of the problems in making this separation.[16a] They used molecular dynamics and semiempirical quantum calculations to obtain a value of $\lambda_{solv} = 3625$ cm^{-1}, which is somewhat smaller than the room-temperature value of 4510 cm^{-1} obtained in this work. Their value contains contributions from the central ring torsions as well as torsions of the peripheral benzene rings. In their gas-phase simulation, where these torsions were the only source of spectral broadening included in the model, LR found a reorganization energy of 760 cm^{-1} and observed the transition to be strongly influenced by the torsions of the central bond between the pyridyl and phenoxide groups. If this torsional contribution is the same in the solution phase spectrum, then LR's predicted value of λ_{solv} would be only 2865 cm^{-1}. However, their simulation of betaine-30 in acetonitrile showed that the transition energy was not highly correlated with this torsion. Thus, the contribution of torsional motions to the total λ_{solv} reported by Rossky et al. should be considerably smaller than 760 cm^{-1}. In this work, the total internal reorganization energy of 120 cm^{-1} includes only 33 cm^{-1} from the central torsion. Our estimate of the torsional contribution to λ_{int} is approximate because we did not determine the full Raman profile for this mode, since it is impossible to determine its cross section against the background due to Rayleigh scattering. Clearly, the low intensity of the 133 cm^{-1} mode is consistent with only a small contribution to λ_{int} from the central torsion, in agreement with ref 16. Mente and Maroncelli[17] (MM) report a λ_{solv} of 4260 cm^{-1}, from Monte Carlo simulations and INDO calculations, which is in good agreement with the present results. This value was calculated for a rigid betaine molecule and so does not include any

contributions from torsions. The value $\lambda_{class} = 1100$ cm^{-1} was obtained by MM from a gas-phase calculation and includes only contributions from the central torsion. This value is also much larger than the total internal reorganization energy obtained in this work. The reorganization energies derived by Barbara and co-workers (ref 2a) were determined by analysis of the line shape of the spectrum of betaine-30 in acetonitrile and the rate of back-electron transfer. The total classical reorganization energy of 3444 cm^{-1} was further partitioned into solvent (2221 cm^{-1}) and internal classical (1223 cm^{-1}) contributions by fitting the absorption line shape in nonpolar solvent and attributing all the classical reorganization to the latter. We conclude that the classical contribution to the reorganization energy is solvent dependent and that the classical contribution to the line width in polar solvent cannot be derived from the line shape of the same solute in nonpolar solution. It has been suggested that the low-frequency internal vibrations may couple to solvent dynamics, leading to solvent dependent[18] (and even solvent isotopomer dependent[3]) values for the "classical" reorganization energy. The internal reorganization energy of 1236 cm^{-1} reported by Barbara et al. was determined by assuming a single high-frequency intramolecular vibration of 1554 cm^{-1}. This value of λ_{int} is larger than the total internal reorganization found in this work, which is due to 19 coupled vibrations rather than a single mode.

A recent report on the femtosecond spectroscopy of betaine-30 in acetonitrile[19] determined a solvent reorganization energy of 2000 cm^{-1} and assigned 1430 cm^{-1} of internal reorganization to a single internal mode at 1350 cm^{-1}. When these values are employed to calculate the Raman intensity of the 1350 cm^{-1} mode at an excitation wavelength of 600 nm, the predicted cross section of about 10^{-9} Å^2 is 2 orders of magnitude larger than the experimental value, and of course, there would be virtually no Raman intensity for any of the other 18 modes in this picture. The rather large value of λ_{int} reported in ref 19 was based on the observation of prompt (~10 fs) stimulated emission with a large red shift compared to the excitation wavelength, which was assigned to fast vibrational relaxation of high-frequency modes. It is not clear how the additive contributions from bleaching, excited-state absorption, and stimulated emission were separated in order to arrive at this conclusion.

The solvent isotope effect on the Raman intensities, and lack of one on the absorption spectrum, forces us to consider nonlinear solvent response—that is, different solvent dynamics couple to the excited electronic state compared to those of the ground state. Without Raman data in both CH_3CN and CD_3CN, it would be impossible to separate the internal and solvent reorganization energies. However, we take advantage of the fact that the internal-mode displacements are independent of solvent isotope. The global analysis of nine Raman excitation profiles in both solvents leads to solvent reorganization energies of 3320 and 3690 cm^{-1} in CH_3CN and CD_3CN, respectively. This corresponds to an amplitude D which is only about 5% larger in deuterated compared to that in protiated acetonitrile. This small difference could be a consequence of the isotope effect on the collision frequency, which is expected to be about 3% higher in CH_3CN than CD_3CN. We speculate that the ~70 fs inertial phase of the solvent is of slightly larger amplitude in deuterated acetonitrile, due to the smaller collision frequency. For most of the modes, this small change in λ_{solv} accounts for the difference in the observed Raman cross sections. The calculated intensity of the 289 cm^{-1} mode, which has been assigned to out-of-plane bending of the phenoxide group,[5] is in good agreement with experiment for CD_3CN solution but falls short for CH_3CN. We speculate that this reflects vibrational dynamics not accounted for by the working equations of time-dependent theory, such as coupling of solvent and internal vibrations and mode-dependent dephasing.

The room-temperature value of λ_{solv}(abs) of 4510 cm^{-1} is larger than the value of λ_{solv}(ram) of 3320 cm^{-1} for CH_3CN solution. These values correspond to an amplitude D of 1360 cm^{-1} in the ground state, which is about 16% larger than the value of 1170 cm^{-1} in the excited electronic state. Our results here are in good agreement with the calculations of Mente and Maroncelli,[17] who simulated the absorption spectrum coupled to both the ground and excited-state charge distributions and obtained a ground-state reorganization energy of 4590 cm^{-1} compared to the excited-state reorganization of 3190 cm^{-1}. Due to the strong dependence of the calculated Raman cross section on the magnitude of solvent reorganization energy, this small departure from linear solvent response is easily observed.

In previous publications,[3] we have speculated that the nonlinear solvent response in betaine-30 is a consequence of the reversal in the direction of the dipole moment in the excited electronic state, which induces solvent motion proceding from a highly nonequilibrium configuration. While the conventional resonance structures which are often drawn to represent the ground and excited states suggest that the ground (μ_g) and excited (μ_e) state dipole moments are antiparallel, semiempirical calculations do not necessarily support this conclusion. The INDO calculations of Mente and Maroncelli[20] found μ_g and μ_e to be parallel. The observed solvatochromism of betaine-30 has been accounted for using continuum theory, with a cavity radius of 6.2 Å and a dipole difference that assumes that μ_g and μ_e are parallel.[21] However, the calculations of Lobaugh and Rossky[16a] found a significant component of the excited-state dipole moment along the direction normal to that of the ground-state dipole moment. A recent report on transient electromagnetic radiation associated with the change in dipole moment of betaine-30 in $CHCl_3$, aligned in an electric field, was interpreted with the assumption that the direction of the excited-state dipole moment is opposite to that of the ground state.[22] Regardless of the uncertainty in the relative direction of the ground and excited-state dipole moments, there is much evidence to support the conclusion that the magnitudes of μ_g and μ_e are quite different, not the least of which is the strong solvatochromism. In addition, femtosecond pump−probe experiments[23] have observed coherent librational motion of the solvent (acetonitrile and dichlorobenzene) in response to excitation of betaine-30. It seems likely that the large change in charge distribution of betaine-30 that accompanies the electronic transition perturbs the solvent dynamics and results in nonlinear response.

It would be very interesting to compare the results of the present study to alternative measurements of temperature dependent solvent relaxation. Fourkas et al. have measured temperature-dependent optical Kerr effect spectra for acetonitrile and found that the collective reorientation time decreases from about 4 to 1 ps as the temperature is raised from 230 to 344 K at constant pressure.[24] Similarly, the intermediate relaxation time, which arises from intermolecular dynamics, drops from 1.1 to 0.34 ps over this temperature range. One would like to compare the time scale Λ^{-1} from this study to the relaxation times from OKE, but unfortunately, the frequency Λ is not well-determined here due to the inhomogeneous limit, $D \gg \Lambda$. However, the temperature trends in both the collective reorientational and intermediate relaxation times are in accord with the qualitative conclusions of the present study: that the solvent structure loosens as the temperature is raised and the solvent becomes effectively less polar.

V. Conclusions

The temperature-dependent absorption spectrum of betaine-30 in acetonitrile has been accounted for using time-dependent spectroscopy theory, and values of the solvent reorganization energy and band origin as a function of temperature have been determined. Simultaneous modeling of the absorption spectrum and nine Raman excitation profiles of betaine-30 in CH_3CN and CD_3CN have enabled the internal and ground and excited state solvent reorganization energies to be determined. Comparison of solvent reorganization energies found from modeling the absorption and Raman profiles reveals significant departure from linear solvent response. For the most part, a small difference in amplitude of the solvent-induced frequency fluctuations, in protiated versus deuterated solvent, accounts for the solvent isotope effect on the Raman intensities. The model fails to account for the large solvent isotope effect on the phenoxide bending motion at 289 cm^{-1}, which may reflect vibrational relaxation or coupling of solvent and solute vibrations not accounted for in the present theory. The reduced amplitude of the solvent response when coupled to the excited rather than the ground state of the solute could be a consequence of the decrease in the dipole moment in the excited state. The potential energy along the solvent coordinate is envisioned to have decreased curvature in the excited compared to the ground electronic state. If this hypothesis is correct, a charge-transfer transition in which the dipole moment increases on excitation might exhibit an increase in solvent reorganization energy in the excited electronic state. Further studies of positively solvatochromic dyes, in which the excited-state dipole moment is larger than the ground, will permit this hypothesis to be tested.

Acknowledgment. Acknowledgment is made to the donors of the Petroleum Research Fund, administered by the ACS, for partial support of this work, and to the National Science Foundation.

References and Notes

(1) Reichardt, C. *Solvent and Solvent Effects in Organic Chemistry*; VCH: Weinheim, Germany, 1990. (b) Reichardt, C. *Chem. Rev.* **1994**, *92*, 2319.

(2) Walker, G. C.; Åkesson, E.; Johnson, A. E.; Levinger, N. E.; Barbara, P. F. *J. Phys. Chem.* **1992**, 96, 3728. (b) Johnson, A. E.; Levinger, N. E.; Jarzeba, W.; Schlief, R. E.; Kliner, D. A. V.; Barbara, P. F. *Chem. Phys.* **1993**, *176*, 555. (c) Reid, P. J.; Barbara, P. F. *J. Phys. Chem.* **1995**, *99*, 3554. (d) Barbara, P. F.; Walker, G. C.; Smith, T. P. *Science* **1992**, *256*, 975.

(3) Zong, Y.; McHale, J. L. *J. Chem. Phys.* **1997**, *106*, 4963. (b) Zong, Y.; McHale, J. L. *J. Chem. Phys.* **1997**, *107*, 2920.

(4) Luzkhov, V.; Warshel, A. *J. Am. Chem. Soc.* **1991**, *113*, 4491. (b) Vath, P.; Zimmt, M. B. *J. Phys. Chem. A* **2000**, *104*, 2626. (c) Vath, P.; Zimmt, M. B.; Matyushov, D. V.; Voth, G. A. *J. Phys. Chem. B* **1999**, *103*, 9130.

(5) Hogiu, S.; Werncke, W.; Pfeiffer, M.; Dreyer, J.; Elsasesser, T. *J. Chem. Phys.* **2000**, *113*, 1587. (b) Hogiu, S.; Dreyer, J.; Pfeiffer, M.; Brzezinka, K.-W.; Werncke, W. *J. Raman Spectrosc.* **2000**, *31*, 797.

(6) Myers, A. B. *Chem. Rev.* **1996**, *96*, 911. (b) Myers, A. B. *Chem. Phys.* **1994**, *180*, 215.

(7) (a) Dimroth, K.; Reichardt, C.; Schweig, A. *Liebigs Ann. Chem.* **1963**, *669*, 95. (b) Laurence, C.; Nicolet, P.; Reichardt, C. *Bull. Soc. Chim. France* **1987**, 125. (c) Kjaer, A. M.; Kristjansson, I.; Ulstrup, J. *J. Electroanal. Chem.* **1986**, *204*, 45.

(8) Yan Y. J.; Mukamel, S. *J. Chem. Phys.* **1986**, *85*, 462. (b) Li, B.; Johnson, A. E.; Mukamel, S.; Myers, A. B. *J. Am. Chem. Soc.* **1994**, *116*, 11039.

(9) Gu, Y.; Widom, A.; Champion, P. M. *J. Chem. Phys.* **1994**, *100*, 2547.

(10) Riddick, J. A.; Bunger, W. B. *Techniques of Chemistry, Vol. II, Organic Solvents, Physical Properties and Methods of Purification*; Wiley-Interscience: New York, 1970.

(11) In *CRC Handbook of Chemistry and Physics*, 80th ed.; D. R. Lide, Ed.; CRC Press: Boca Raton, FL, 1999.

(12) Golini, G. M.; Williams, B. W.; Foresman, J. B. *J. Fluoresc.* **1998**, *8*, 395.

(13) Brunschwig, B. S.; Ehrensen, S.; Sutin, N. *J. Phys. Chem.* **1987**, *91*, 4714.

(14) Liptay, W.; Dumbacher, B.; Weisenberger, H. *Z. Naturforschung, Teil A* **1968**, *23*, 1613.

(15) (a) Heller, E. J.; Sundberg, R. L.; Tannor, D. *J. Phys. Chem.* **1982**, *86*, 1822. (b) Lee, S.-Y.; Heller, E. J. *J. Chem. Phys.* **1979**, *71*, 4777. (c) Myers, A. B.; Mathies, R. A. In *Biological Applications of Raman Spectroscopy*; Spiro, T., G., Ed.; Wiley: New York, 1987; Vol. 2, p 1.

(16) (a) Lobaugh, J.; Rossky, P. J. *J. Phys. Chem. A* **2000**, *104*, 899. (b) Ishida, T.; Rossky, P. J. *J. Phys. Chem. A* **2001**, *105*, 558.

(17) Mente, S. R.; Maroncelli, M. *J. Phys. Chem. B* **1999**, *103*, 7704.

(18) Matyushov, D. V.; Schmid, R.; Ladanyi, B. M. *J. Phys. Chem. B* **1997**, *101*, 1035.

(19) Kovalenko, S. A.; Eilers-König, N.; Senyushkina, T. A.; Ernsting, N. P. *J. Phys. Chem. A* **2001**, *105*, 4834.

(20) Maroncelli, M. Personal communication, 1999.

(21) Ravi, M.; Samanta, A.; Radhakrishnan, T. P. *J. Phys. Chem.* **1994**, *98*, 9133.

(22) Beard, M. C.; Turner, G. M.; Schmuttenmaer, C. A. *J. Am. Chem. Soc.* **2000**, *122*, 11541.

(23) McElroy, R.; Wynne, K. *Phys. Rev. Lett.* **1997**, *79*, 3078.

(24) Loughnane, B. J.; Scodinu, A.; Farrer, R. A.; Fourkas, J. T. *J. Chem. Phys.* **1999**, *111*, 2686.